

Critical currents of small $\text{Bi}_2\text{Sr}_2\text{CaCu}_2\text{O}_{8+x}$ intrinsic Josephson junction stacks in external magnetic fields

A. Irie,¹ S. Heim,² S. Schromm,³ M. Möhle,² T. Nachtrab,³ M. Gódo,³ R. Kleiner,² P. Müller,³ and G. Oya¹

¹*Department of Electrical and Electronic Engineering, Utsunomiya University, Utsunomiya 321, Japan*

²*Physikalisches Institut-Experimentalphysik II, Universität Tübingen, Auf der Morgenstelle 14, D-72076 Tübingen, Germany*

³*Physikalisches Institut III, Universität Erlangen-Nürnberg, D-91058 Erlangen, Germany*

(Received 7 February 2000)

We present a study of the critical currents of small sized intrinsic Josephson junction stacks in external magnetic fields applied parallel to the CuO_2 layers. The stacks consisting of 5–12 junctions were realized as mesa structures patterned on top of $\text{Bi}_2\text{Sr}_2\text{CaCu}_2\text{O}_{8+x}$ single crystals. Lateral mesa dimensions ranged from 10×10 to $0.8 \times 0.8 \mu\text{m}^2$. For the largest structures a complex magnetic field dependence of the critical currents was found. With decreasing mesa dimensions the critical currents systematically approached a Fraunhofer-type magnetic field dependence. Measurements agree well with the results of numerical calculations using coupled sine-Gordon equations.

I. INTRODUCTION

One of the most characteristic manifestations of the Josephson effect is the Fraunhofer-like magnetic field dependence of the maximum supercurrent across a small rectangular Josephson junction $I_c(B) = I_c(0) |\sin(\pi B/B_0)/(\pi B/B_0)|$. Here, the external field B is oriented parallel to the junction barrier. B_0 is given by the ratio of the flux quantum Φ_0 to the effective area of the junction, determined by the junction width b perpendicular to the applied field and the effective junction thickness t_{eff} . In order to achieve Fraunhofer-like pattern the junction dimensions should not exceed the Josephson length λ_J , and the junction should be homogeneous. For a conventional Josephson junction with superconducting electrodes much thicker than the London penetration depth λ_L , the Josephson length is given by $[\Phi_0/2\pi\mu_0j_c(2\lambda_L + \bar{t})]^{1/2}$ with the barrier thickness \bar{t} and the critical current density j_c . Typically, λ_J amounts several μm . The effective junction thickness t_{eff} is given by $2\lambda_L + \bar{t}$ yielding values of B_0 on the order of some Gauss. Thus the conditions to observe the Fraunhofer pattern can be realized easily, and measurements of I_c vs B are routinely used to characterize the homogeneity of artificially made Josephson junctions. In contrast, for intrinsic Josephson junctions in high temperature superconductors formed by adjacent CuO_2 double layers,¹ it has turned out to be notoriously difficult to approach the conditions necessary to observe a Fraunhofer pattern. The main reason is that for this kind of junctions the thickness d of the superconducting layers is only 3 Å, much less than the (in-plane) London penetration depth $\lambda_{ab} \approx 1500$ Å. The large kinetic moment of supercurrents flowing along a superconducting layer give rise to a modified Josephson length $\lambda_J \approx (\Phi_0 d / 4\pi\mu_0 j_c \lambda_{ab}^2)^{1/2}$, which, for a typical critical current density of 10^3 A/cm², is only about 0.4 μm . Furthermore, these circulating currents strongly couple adjacent junctions. Still, however, the junctions forming the stack can be individually switched to their resistive state. Ideally one would like to monitor the critical current of every individual junction which is virtually impossible if the

stack consists of, say, 100 junctions. An adequate discussion of the intrinsic Josephson effect thus requires small sized stacks consisting of as few as possible junctions. These requirements can be approached with present day fabrication technologies.

The dynamics of intrinsic junction stacks is believed to be adequately described by the coupled sine Gordon equations which can be derived from either the Lawrence-Doniach model for layered superconductors^{2–4} or by generalizing the sine Gordon equation for a single Josephson junction to a system of stacked junctions^{5,6}. An analysis of these equations shows that, when the lateral dimensions of the stack are below λ_J , the critical current of each junction follows a Fraunhofer pattern with $B_0 = \Phi_0 / [(\bar{t} + d)b]$.³ For $\text{Bi}_2\text{Sr}_2\text{CaCu}_2\text{O}_8$ (BSCCO) the thickness $\bar{t} + d$ of an intrinsic Josephson junction equals 15 Å. For a width of the stack of $b = 0.5 \mu\text{m}$ the first zero of the Fraunhofer pattern would occur at $B_0 = 2.76$ T. On such field scales sample alignment becomes crucial in order to avoid the formation of pancake vortices penetrating the superconducting layers. For example, in order to keep the perpendicular field component below 20 G in a 2 T field the misalignment needs to be less than 0.06° .

Early measurements of I_c vs B have been performed on small single crystals of $30 \times 30 \mu\text{m}^2$ or larger in size consisting of more than 1000 junctions.¹ The critical current of the weakest junction exhibited shallow modulations on field scales corresponding to a flux quantum per junction but saturated on a level of more than 50% per cent of its zero field value. Similar modulations have been found for BSCCO single crystal whiskers with lateral sizes between 20 and 40 μm .^{7,8} For such structures a systematic study of I_c vs B was carried out.⁹ Structures with lateral dimensions ranging from 8 μm to 200 μm consisting of about 100 stacked junctions have been studied. I_c vs B of the smallest structure showed pronounced oscillations. A crossover from an oscillatory, size dependent behavior of I_c to a size-independent decrease of I_c , as predicted by Fistul and Giuliani,¹⁰ was found for a junction width of about 20–30 μm . The pronounced oscillations found for the smallest structures may

perhaps be surprising since this structure was still five times larger than λ_J .¹¹ For 1.2 μm wide whisker structures having a hole in the center, recently a Fraunhofer-like pattern for the weakest junction of the stack was reported.¹²

Intrinsic junction stacks consisting of less than 100 junctions can be realized as mesa structures on top of BSCCO single crystals.^{13,14} In this geometry, with mesa sizes between 10 and 50 μm , I_c vs B of the weakest junction has been measured by several authors.^{15–17} In fields up to several T I_c decreased strongly but no pronounced oscillations were found.

A systematic investigation of I_c vs B of small intrinsic junction stacks consisting of a small number of junctions is clearly necessary. The main question is if and how the Fraunhofer pattern develops when the mesa size is decreased. In this paper we present data for mesa structures patterned on top of single crystals. The mesas consisted of between 5 and 12 junctions. Their lateral sizes were between $10 \times 10 \mu\text{m}^2$ and $0.8 \times 0.8 \mu\text{m}^2$. The small junction number allowed to monitor the critical currents of all junctions in the stack. We will discuss the transition to the short junction limit and will compare our results with numerical solutions of the coupled sine-Gordon equations.

II. EXPERIMENTS

BSCCO single crystals were grown from a stoichiometric mixture of the oxides and carbonates. They were grown at either Erlangen University¹⁸ or Utsunomiya University.¹⁹ X-ray diffraction confirmed that the crystals were single phase. The bulk transition temperature of the as grown crystals was about 88 K. For the experiments single crystals of approximately $1 \times 1 \times 0.1 \text{ mm}^3$ in size were selected. Epoxy was used to glue the crystals to a sapphire substrate. To obtain a sufficiently small contact resistance the crystals were cleaved immediately before mounting them into the vacuum chamber and the crystal surface was covered with silver. The contact resistance was typically $10^{-5} \Omega \text{ cm}^2$. Subsequently, quadratic mesa structures with lateral dimensions down to 0.8 μm were patterned using electron beam lithography and argon-ion milling. For electrical insulation of the lead contacting the top of the mesa a 250 nm thick SiO layer was evaporated. The top contact was provided by a 300–400 nm thick gold or silver layer. Currents were extracted from the base crystal using large pads contacting its top surface. The leads and contact pads were patterned by photolithography and argon-ion milling. Transport measurements were performed in a two-terminal configuration. Low pass filters were used to reduce external noise and the bias current was provided by a battery powered current source. Current-voltage (I - V) characteristics were recorded by digital voltmeters. Temperatures could be varied between room temperature and 4.2 K. Magnetic fields were applied by either a 5 T superconducting split coil magnet or a 0.9 T superconducting Helmholtz coil. The field orientation relative to the CuO_2 layers could be adjusted to an accuracy of 0.01° .

III. RESULTS

We start with results for the $10 \times 10 \mu\text{m}^2$ mesa SH16. Representative parameters for this and all other mesas dis-

TABLE I. Various parameters of the mesa structures used.

Sample	Size [μm^2]	Junction number	j_c [A/cm^2]	b/λ_J
SH16	10×10	10	800	20
SH120	2×2	7	5000	10
Aph3	2×2	8	1000	5
3–9	1.2×1.2	12	170	1.2
SH146	0.8×0.8	7	1700	2.7

cussed are listed in Table I. Mesa SH16 consisted of eight junctions. At $T = 10 \text{ K}$ the critical currents of the eight junctions ranged between 0.8 and 0.9 mA. Assuming $\lambda_{ab} = 1500 \text{ \AA}$ the Josephson length was about 0.47 μm corresponding to a ratio b/λ_J of more than 20. This stack was thus far from the short junction limit. In order to align the sample relative to the external field we made use of the fact that the critical currents get strongly suppressed due to the formation of pancake vortices when the external field has some misorientation angle away from the parallel orientation. When measured at high enough temperatures the field induced changes of the I - V characteristics were reversible and could be used for alignment, as shown in Fig. 1 (center). Here, $T = 55 \text{ K}$ and $B = 3.6 \text{ kG}$. The sample was biased at a current of 96 μA and the resistance change was monitored while the angle Θ between the external field and the layers was rotated by 180° . For perpendicular orientation ($\Theta = 90^\circ$) the critical currents were completely suppressed and a large resistance was monitored. For decreasing angle, I_c became larger leading to a decreased resistance with a minimum value at Θ

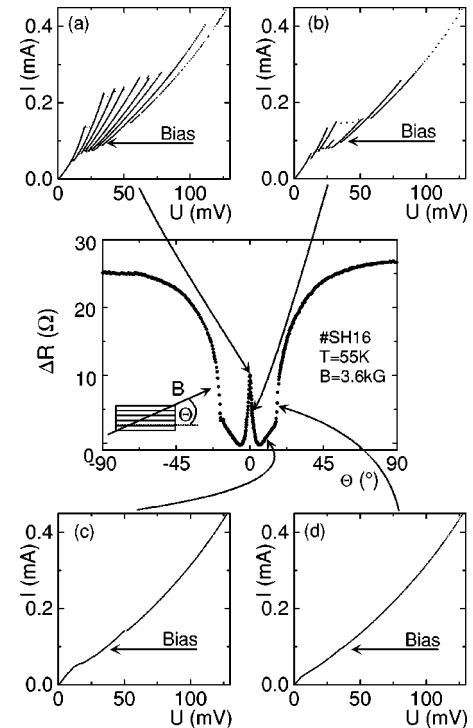


FIG. 1. Resistance of $10 \times 10 \mu\text{m}^2$ mesa SH16 vs orientation angle of external field Θ (center figure). Bias current was set to 96 μA . Figures labeled (a) to (d) show current voltage characteristics for several values of Θ ; (a) $\Theta = 0^\circ$, (b) $\Theta = 2^\circ$, (c) $\Theta = 7^\circ$, and (d) $\Theta = 18^\circ$.

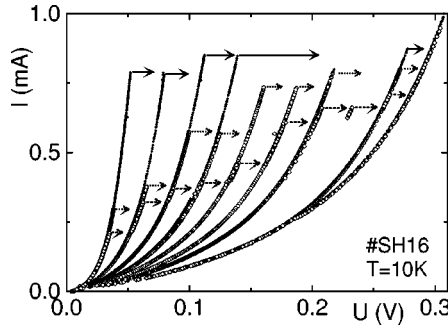


FIG. 2. Current-voltage characteristic of $10 \times 10 \mu\text{m}^2$ mesa SH16 at $T=10$ K, as measured at $B=0$ (solid circles), $B=1.47$ kG (open circles), and $B=2.88$ kG (diamonds). Arrows indicate switching to larger voltages at $B=0$ (solid arrows), 1.47 kG (dotted arrows), and 2.88 kG (dashed arrows). Note that some branches are stable only in nonzero magnetic fields.

$=6^\circ$. For smaller angles the resistance sharply increased due to Josephson fluxons moving through the stack.²⁰ The effect of misalignment on the I - V characteristics and the critical currents of the individual junctions can be clearly seen from Figs. 1(a)–1(d) showing I - V characteristics at, respectively, $\Theta=0^\circ, 2^\circ, 7^\circ$ and 18° . Note that there is already a large resistance at low bias currents which is not due to the contact resistance to the uppermost CuO_2 layer but due to a degraded surface junction.^{21,22} A misalignment of 2° was sufficient to suppress the critical currents by a factor of 2 [Fig. 1(b)].

When $\Theta=0^\circ$ was adjusted within an accuracy of $\pm 0.01^\circ$ the temperature was first increased above T_c and then lowered to 10 K to measure I_c vs B . Figure 2 shows the I - V characteristics at 10 K in zero magnetic field (solid circles), as well as for external fields of 1.47 kG and 2.8 kG, corresponding to ratios of B/B_0 of 1.07 and 2.03. Arrows indicate switching to larger voltages occurring when the critical current of one of the junctions is exceeded. While at $B=0$ all junctions switched in a narrow interval between 0.8 and 0.87 mA the distribution of critical currents became much larger for $B=1.47$ kG where the first junction switched at a current of 0.3 mA, whereas the last junction switched at 0.8 mA. For $B=2.8$ kG the weakest junction switched at 0.2 mA and the last junction switched at 0.7 mA.

Figure 3(a) shows I_c vs B for all junctions in the stack as determined from the voltage jumps in the I - V characteristics. With this definition the lowest I_c corresponds to the true critical current of the stack while the critical currents of the other junctions are determined for some other of junctions already being resistive. Different symbols in the figure mark the different resistive branches. Note, however, that a given branch number does not necessarily correspond to always the same junction within the stack. From the I - V characteristics one can infer the number of junctions, corresponding to the number of resistive branches, but not the location of individual junctions within the stack. An exception is possibly the first branch with the weakest critical current, which is most likely the outermost junction of the stack.

I_c of the weakest junction (solid circles) dropped on a scale of B_0 (corresponding to 1.38 kG) and then tended to level out. A similar behavior was observed for the second branch (open circles). In contrast, the three outermost branches

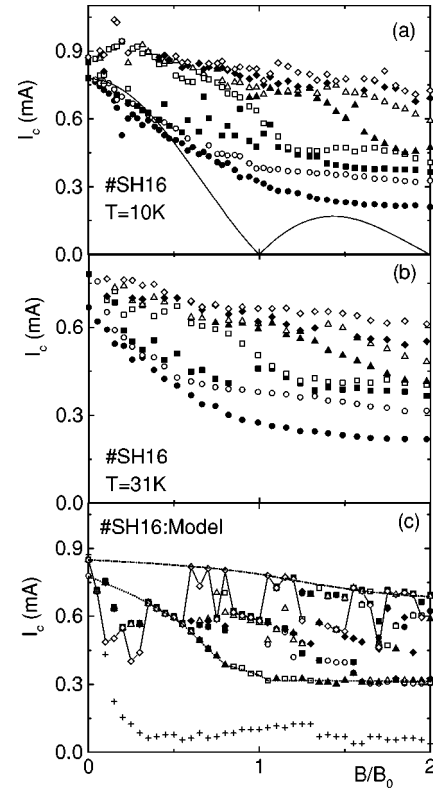


FIG. 3. Magnetic field dependence of the critical currents of the eight junctions of $10 \times 10 \mu\text{m}^2$ mesa SH16 at (a) 10 K and (b) 31 K. Symbols label branch numbers 1 to 8 as solid and open circles, solid and open squares, solid and open triangles, and solid and open diamonds. (c) shows I_c vs B of $10 \mu\text{m}$ wide eight junction stack, as calculated from coupled one-dimensional sine-Gordon equations for parameters of sample SH16 at 10 K. Symbols denote outermost junction 1 to junction 8 located next to base crystal in same notation as in (a). Crosses mark I_c of uppermost dummy junction modelling base crystal. Solid line in (a) is Fraunhofer pattern. Dashed and dotted lines in (c) are guides to the eye. $B_0=1.38$ kG. For one junction unstable switching behavior is demonstrated by connecting symbols (diamonds) with solid lines.

(open and closed diamonds, open triangles) -showed some weak modulations but decreased only slightly up to a field of $2B_0$. I_c of the intermediate branches either behaved instable (solid squares) or exhibited some stronger modulation (open squares and solid triangles). The observed behavior is similar to earlier measurements of I_c of $30 \times 30 \mu\text{m}^2$ sized single crystals mounted between contact rods.^{1,6} In any case, $I_c(B)$ is far from a Fraunhofer pattern which is shown as solid line matched to the expected first zero of the weakest junction. When repeating the measurement at the same or even a higher temperature there was little change in the data, as shown in Fig. 3(b) for sample SH16 at $T=31$ K. Qualitatively similar data were also obtained for another $10 \times 10 \mu\text{m}^2$ mesa with a ratio b/λ_J of 17 (sample SH21, not shown).

In order to provide deeper understanding we performed calculations using the coupled sine Gordon equations.⁵ The CuO_2 planes are assumed to lie in the xy plane and the magnetic field is applied along y . The width of the stack in field direction is neglected. Its width along x is b . In this geometry, the equations read

$$\frac{\partial^2 \gamma_n}{\partial x^2} \equiv \gamma_n'' = \frac{1}{\lambda_m^2} \frac{j_{z,n}}{j_c} + \frac{1}{\lambda_k^2} \frac{2j_{z,n} - j_{z,n-1} - j_{z,n+1}}{j_c}, \quad (1)$$

with $j_{z,n} = j_{c,n} \sin \gamma_n + \sigma E_{z,n} + \epsilon \epsilon_0 \dot{E}_{z,n}$. Here, n labels the n th junction in the stack, and γ_n is the gauge invariant phase difference of the n th Josephson junction. Bias current is applied in the z direction. The lengths λ_m and λ_k are, respectively, given by $[\Phi_0/2\pi\mu_0 j_c(\bar{t}+d)]^{1/2}$ and $(\Phi_0 d/2\pi\mu_0 j_c \lambda_L^2)^{1/2}$. The Josephson length is given by $(\lambda_m^2 + 2\lambda_k^2)^{-1/2} \approx \lambda_k/\sqrt{2}$. The external field appears via the boundary condition $\partial\gamma_n(x=0)/\partial x = \partial\gamma_n(x=b)/\partial x = 2\pi B_{\text{ext}}(\bar{t}+d)/\Phi_0$. For a numerical solution, Eq. (1) was expanded into spatial Fourier components as described in Ref. 6. We used 32 Fourier components for the 10 μm long stack. Critical current densities were used as measured in zero magnetic field. Since, from the experimental data, we cannot determine to which spatial junction positions the measured critical current correspond, we somewhat arbitrarily assigned the weakest critical current to the outermost junction and sorted the other junctions by increasing critical current. All other junction parameters were assumed to be equal. The displacement current was characterized by the McCumber parameter $\beta_c = 2\pi j_c \epsilon \epsilon_0 \bar{t} / \Phi_0 \sigma^2$, which was set to 50. In order to determine the maximum supercurrent of each junction in the stack at a given field the bias current was increased monotonically from zero. The dc voltage across each junction was monitored and the critical current of each junction was defined by the voltage criterion $U/I_c R_n > 0.05$. In the experiments the mesa structures are formed on a large base crystal which we could not take into account explicitly. In the simulations shown in Fig. 3(c) we approximated the base crystal with two dummy junctions. The junction located next to the base crystal had the same parameters as the adjacent mesa junction, and the other dummy junction had a lower electrode of 3 nm thickness and a critical current ten times larger than the mesa junctions. We also performed simulations where the dummy junction with the thick electrode was replaced by 10 junctions with 3 Å thick electrodes. Both methods yielded similar results.

The simulated curves of Fig. 3(c) are made for the parameters of sample SH16 at $T=10$ K. They agree with the measurements at least on a qualitative level. From these simulations the observed splitting of critical currents with increasing field can essentially be understood by a nonuniform distribution of magnetic flux through the formation of vortex lines in some junctions. Particularly, most fluxons tended to be concentrated in the dummy junction located next to the mesa. For $B/B_0 < 0.3$ the mesa junctions switched to the resistive state through a complex formation of many fluxons and antifluxons. For larger fields, in addition to the fluxon line in the dummy junction, lines of fluxons formed in some of the mesa junctions while the other junctions stayed free of fluxons. The critical current of the junctions containing the fluxon rows was strongly decreased while the critical current of the other junctions stayed on a relatively high value. For a given field, fluxon rows did not always form in the same junctions. As a consequence, each junction could have various values of I_c . Such multiple valued critical currents have been observed recently by Mros *et al.*²² Note,

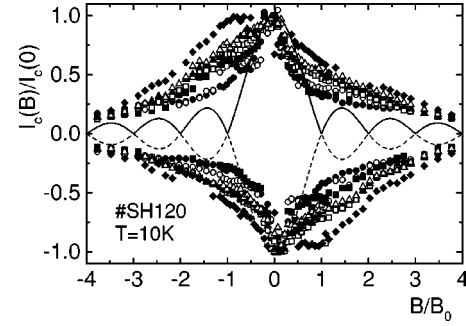


FIG. 4. Magnetic field dependence of the normalized critical currents of the seven junctions of $2 \times 2 \mu\text{m}^2$ mesa SH120 for both polarities of bias current and magnetic field. Josephson length is about 0.2 μm . Different symbols correspond to different branch numbers in same notation as in Fig. 3. Lines correspond to Fraunhofer pattern. $B_0 = 6.9$ kG.

however, that at a given field the various fluxon configurations resulted in very similar sets of critical currents (I_{c1}, \dots, I_{c8}) such that more or less continuous curves $I_c(B)$ [e.g., the dashed and dotted lines Fig. 3(c)] could be obtained. A more detailed classification of the fluxon states found is beyond the scope of this paper and will be given elsewhere.²³

We now turn to results obtained for two $2 \times 2 \mu\text{m}^2$ mesas fabricated on different crystals. Mesa SH120 consisted of seven junctions having critical currents between 160 and 220 μA at $T=10$ K, corresponding to critical current densities between 4 and 5.5 kA/cm^2 . For these junctions, λ_J ranged between 0.18 and 0.2 μm yielding a ratio b/λ_J of about 10. Thus the mesa was again far from the short junction limit. Figure 4 shows the normalized critical currents of all junctions vs B/B_0 , with $B_0 = 6.9$ kG. Critical currents have been evaluated both for positive and negative bias currents, as well as for both polarities of the magnetic field. Qualitatively, the curves do not differ strongly from the curves measured for the $10 \times 10 \mu\text{m}^2$ mesa, although the normalizing field B_0 is 5 times larger. There was a pronounced asymmetry between the critical currents for positive and negative bias current. Similar asymmetry has been found also for the larger mesas. When the magnetic field was applied with reversed polarity the asymmetry in I_c was also reversed, i.e., one has the case of point symmetry $|I_c(B, I)| = |I_c(-B, -I)|$, showing that the asymmetry is not due to trapped flux but due to asymmetries in bias current which is extracted asymmetrically from the mesa via the base crystal.

For the other $2 \times 2 \mu\text{m}^2$ mesa, sample Aph3, critical currents at 10 K and zero magnetic fields ranged between 38 and 42 μA , and λ_J was about 0.4 μm . The ratio b/λ_J was about 5. Figure 5(a) shows the normalized critical currents vs B/B_0 . For this sample, the critical currents of all junctions followed nearly the same curve and almost no asymmetry was observable. However, Fraunhofer oscillations did not appear. Figure 5(b) shows simulated curves for the junction parameters of sample Aph3 at 10 K. The simulated curves are similar to the measurements, although some weak oscillations in I_c vs B appear at large fields. Also, in a field of about B_0 all critical currents exhibit a sudden drop. This drop occurred when fluxons were present in some of the junctions already at zero or low bias currents. The simulations have been performed in the absence of noise. It seems likely that

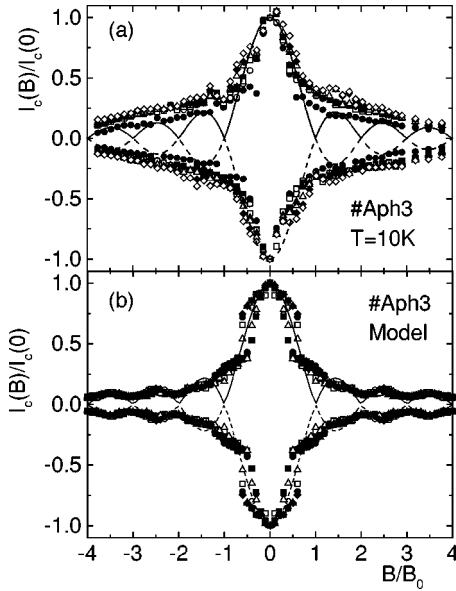


FIG. 5. (a) Magnetic field dependence of the normalized critical currents of the eight junctions of $2 \times 2 \mu\text{m}^2$ mesa Aph3 for both polarities of bias current and magnetic field. Josephson length is about $0.4 \mu\text{m}$. Different symbols correspond to different branch numbers in same notation as in Fig. 3(a). $B_0 = 6.9 \text{ kG}$. Lines correspond to Fraunhofer pattern. (b) Magnetic field dependence of critical currents of $10 \mu\text{m}$ wide eight junction stack, as calculated from coupled one-dimensional sine-Gordon equations for the parameters of Aph3. Symbols label junctions in same notation as in Fig. 3(c).

noise would smear out the above features resulting in a very close agreement with the measured data.

Finally, Figs. 6 and 7 show data for a $1.2 \times 1.2 \mu\text{m}^2$ mesa, sample 3-9, and for a $0.8 \times 0.8 \mu\text{m}^2$ mesa, sample SH146. Even for these small mesa dimensions, the current-voltage characteristics consisted of well defined resistive branches. Sample 3-9 consisted of 12 junctions. The critical current of the weakest junction was about $1.1 \mu\text{A}$ and seven junctions had critical currents of $2.4 \mu\text{A}$, corresponding to $j_c \approx 170 \text{ A/cm}^2$. The critical currents of the other junctions were somewhat larger, between 3.3 and $6.3 \mu\text{A}$. For the Josephson length of the junctions with $2.4 \mu\text{A}$ critical current one obtains a value of $1 \mu\text{m}$. The stack was thus close to the

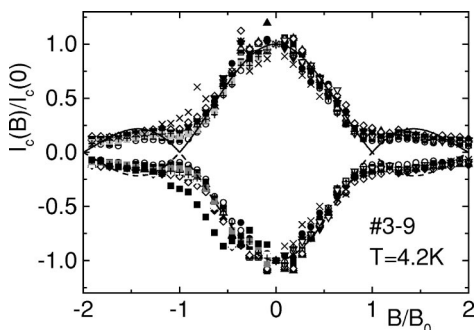


FIG. 6. Magnetic field dependence of the normalized critical currents of the 12 junctions of $1.2 \times 1.2 \mu\text{m}^2$ mesa 3-9 for both polarities of bias current and magnetic field. Josephson length is about $1 \mu\text{m}$. Symbols for branch numbers 1 to 8 are labeled as in Fig. 3(a), higher branches are labeled with solid down triangle (9), open down triangle (10), + (11) and \times (12). Lines correspond to Fraunhofer pattern. $B_0 = 1.1 \text{ T}$.

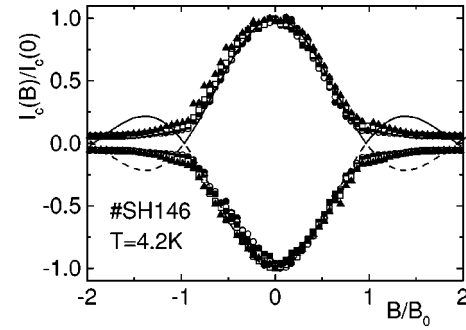


FIG. 7. Magnetic field dependence of the normalized critical currents of the five junctions of $0.8 \times 0.8 \mu\text{m}^2$ mesa SH146 for both polarities of bias current and magnetic field. Josephson length is about $0.3 \mu\text{m}$. Symbols for branch numbers 1 to 5 are labeled as in Fig. 3(a). Lines correspond to Fraunhofer pattern. $B_0 = 1.73 \text{ T}$.

short junction limit. The $0.8 \times 0.8 \mu\text{m}^2$ stack consisted of five junctions with critical currents between 10 and $12 \mu\text{A}$, corresponding to $j_c \approx 1.7 \text{ kA/cm}^2$ and $\lambda_J \approx 0.3 \mu\text{m}$. The ratio b/λ_J was about 2.7 , i.e., more than a factor of 2 larger than the ratio obtained for the $1.2 \times 1.2 \mu\text{m}^2$ mesa. $I_c(B)$ clearly exhibits side maxima which, however, do not agree well with the Fraunhofer pattern. In contrast, for sample 3-9 $I_c(B)$ of all junctions was close to the Fraunhofer pattern showing that the short junction limit can be achieved when the ratio b/λ_J approaches unity. Unfortunately, due to the low absolute values of the critical current of about $0.5 \mu\text{A}$ for fields near B_0 , the Josephson coupling energy is already close to the thermal energy at the temperature of measurement. From this it becomes clear that, in order to reach the small junction limit, the required small geometric dimensions also require very low bath temperatures for stable operation.

IV. SUMMARY

We have studied the magnetic field dependence of the critical currents of all junctions in stacks of intrinsic Josephson junctions with lateral dimensions between 10 and $0.8 \mu\text{m}$. The mesas consisted of only 5–12 junctions. While for large stacks a very complex, although reproducible behavior was found, there is a clear transition to a Fraunhofer pattern as soon as the lateral dimensions of the stack approach the Josephson length. The measurements also showed that precise sample alignment is crucial to obtain reliable data. All measurements agreed well with the results of numerical calculations using coupled sine-Gordon equations showing that these equations provide the proper frame to describe the physics of intrinsic junction stacks.

ACKNOWLEDGMENTS

The authors would like to thank A. V. Ustinov and O. Waldmann for valuable discussions. We gratefully acknowledge financial support by the Bayerische Forschungsstiftung, by the Deutsche Forschungsgemeinschaft, and by a Grant-in-Aid for Scientific Research from The Ministry of Education, Science, Sports and Culture of Japan, and CREST (Core Research for Evolutional Science and Technology) of Japan Science and Technology Corporation (JST).

- ¹R. Kleiner, F. Steinmeyer, G. Kunkel, and P. Müller, *Phys. Rev. Lett.* **68**, 2394 (1992); R. Kleiner and P. Müller, *Phys. Rev. B* **49**, 1327 (1994).
- ²J.R. Clem, and M.W. Coffey, *Phys. Rev. B* **42**, 6209 (1990).
- ³L.N. Bulaevskii, J.R. Clem, and L.I. Glazman, *Phys. Rev. B* **46**, 350 (1992).
- ⁴L.N. Bulaevskii, M. Zamora, D. Baeriswyl, H. Beck, and J.R. Clem, *Phys. Rev. B* **50**, 12 831 (1994).
- ⁵S. Sakai, P. Bodin, and N.F. Pedersen, *J. Appl. Phys.* **73**, 2411 (1993).
- ⁶R. Kleiner, P. Müller, H. Kohlstedt, N.F. Pedersen, and S. Sakai, *Phys. Rev. B* **50**, 3942 (1994).
- ⁷Yu.I. Latyshev and J.E. Nevelskaya, *Physica C* **235**, 2291 (1994).
- ⁸F. Hamed, S. Gygax, and A.E. Curzon, *Physica C* **293**, 280 (1997).
- ⁹Yu.I. Latyshev, J.E. Nevelskaya, and P. Monceau, *Phys. Rev. Lett.* **77**, 932 (1996).
- ¹⁰M.V. Fistul and G.F. Giuliani, *Physica C* **230**, 9 (1994).
- ¹¹S.E. Shafranjuk and T. Yamashita, *Phys. Rev. B* **58**, 121 (1998).
- ¹²Yu.I. Latyshev, V.N. Pavlenko, S.-J. Kim, and T. Yamashita (unpublished).
- ¹³F.X. Régi, J. Schneck, J.F. Palmier, and H. Savary, *J. Appl. Phys.* **76**, 4426 (1994).
- ¹⁴A. Yurgens, D. Winkler, N.V. Zavaritsky, and T. Claeson, *Phys. Rev. B* **53**, R8887 (1996).
- ¹⁵M. Suzuki, T. Watanabe, and A. Matsuda, *Phys. Rev. Lett.* **81**, 4248 (1998).
- ¹⁶A. Yurgens, D. Winkler, T. Claeson, G. Yang, I.F.G. Parker, and C.E. Gough, *Phys. Rev. B* **59**, 7196 (1999).
- ¹⁷V.M. Krasnov, N. Mros, A. Yurgens, and D. Winkler, *Phys. Rev. B* **59**, 8463 (1999).
- ¹⁸W. Gerhäuser, H.W. Neumüller, W. Schmitt, G. Ries, G. Saemann-Ischenko, H. Gerstenberg, and F.M. Sauerzopf, *Physica C* **185**, 2273 (1991).
- ¹⁹A. Irie, M. Sakakibara, and G. Oya, *IEICE Trans. Electron.* **E77-C**, 1191 (1994).
- ²⁰G. Hechtfischer, R. Kleiner, K. Schlenga, W. Walkenhorst, P. Müller, and H.L. Johnson, *Phys. Rev. B* **55**, 14 638 (1997).
- ²¹N. Kim, J. Doh, H.-S. Chang, and H.-J. Lee, *Phys. Rev. B* **59**, 14 639 (1999).
- ²²N. Mros, V.M. Krasnov, A. Yurgens, D. Winkler, and T. Claeson, *Phys. Rev. B* **57**, R8135 (1998).
- ²³R. Kleiner, T. Gaber, and G. Hechtfischer (unpublished).